P4.18 Drizzle Detection for Maritime Stratocumulus Clouds by Combined Use of TRMM Microwave Imager and Visible/Infrared Scanner

Hongfei Shao* and Guosheng Liu
Florida State University, Tallahassee, FL 32306

1. INTRODUCTION

Determining the radiative effects of aerosols is currently one of the most active areas in climate research. Evidences demonstrate that aerosols can affect the radiative balance of the Earth by influencing cloud properties. Aerosols act as condensation nuclei that form clouds. As the number of aerosols increases, the water in the cloud gets spread over many more particles. Large concentrations of small droplets make these clouds more reflective, and reduce the effectiveness of coalescence at a later stage of cloud development through narrowing the spectrum of droplet size, then prolong cloud lifetimes. This indirect effect - increased number concentration of cloud droplets and prolonged cloud lifetime - are believed to have a great impact on global climate. Precipitation is a key component in determining the lifetime and extent of clouds. It also is a key component in the atmospheric energy balance through the redistribution of latent heat. Therefore understanding to what extent that drizzle is suppressed in the polluted cloud is essential for us to assess aerosol indirect effect. Although drizzles have been observed by aircraft and surface-based cloud radars, they can hardly be detected by satellite sensors, which cover much broader area and much longer time period than aircraft or surface based measurements. As a first step in assessing aerosol-induced effect on suppression of precipitation, in this study, we formulate a drizzle detection index - Scale Re, based on satellite microwave and visible/infrared measurements.

2. SCALE Re

One of the key variables that determine the radiative properties of liquid water clouds and reflect the aerosol indirect effect is the cloud effective radius Re (Hansen and Travis 1974), which is defined as the ratio of the third to the second moment of a droplet size distribution n(r), i.e.,

$$\mathrm{Re} = \frac{\int_0^\infty r^3 n(r) dr}{\int_0^\infty r^2 n(r) dr} \qquad (1)$$

* Corresponding author address: Hongfei Shao Florid State University, Dept. of Meteorology, Tallahassee, Florida 32310; email:soar@met.fsu.edu

Presently, space-borne passive sensors are capable of deriving the effective radius of clouds from two distinct methods. The first method makes use of solar reflectance measurements at nonabsorbing visible and absorbing near-infrared frequencies to determine the cloud visible optical depth (τ) and the effective radius of the cloud droplets [hereafter referred to as Re(SR)]. The second approach uses liquid water path (LWP) from microwave and cloud optical depth from visible measurements to infer effective radius [hereafter referred to as Re(MW)] according to the relationship (see Fig.1):

$$LWP = \frac{2}{3}\tau \cdot \mathrm{Re} \qquad (2)$$

The main differences between these two methods are: Re(SR) tends to be biased toward an effective radius somewhere near cloud top while Re(MW) is a measurement of an average droplet radius over the whole cloud layer. Because Re(SR) retrieval relies on absorption at the near-infrared, photons at this frequencies do not penetrate clouds as deep as those at microwave and visible frequencies. On the other hand, Re(MW) is derived from LWP and τ; both of them are integral quantities of the cloud.

The difference between Re(SR) and Re(MW) is therefore able to reflect the vertical inhomogeneity of particle size inside the cloud. For example, if Re(SR) > Re(MW), it indicates that the effective radii increase with height; if Re(MW) < Re(SR), a profile that effective radii decrease with height could be inferred. Generally, for a warm cloud, 1) at the cloud formation stage cloud droplets grow by condensation, effective radius increases with height and reaches a maximum near the top; 2) at precipitation formation stage relatively large droplets (larger than 20 micrometers in radius) fall through the cloud and grow by coalescence, then effective radius increase with the decrease of height and reach a maximum near or below the cloud base. That is, for non-precipitating clouds the ratio of Re(MW) to Re(SR) is less than unity, while for the precipitating clouds the ratio exceeds unity. Therefore, we introduce a scaled Re as drizzle index [hereafter referred to as Re(DI)] to discriminate whether a cloud is precipitating or not:

$$\mathrm{Re}(DI) = \frac{\mathrm{Re}(MW)}{\mathrm{Re}(SR)} \cdot \mathrm{Re}(MW) \qquad (3)$$

Re(DI) consists of two terms: 1) the second term

of the right hand of Eq.(3) is rainfall information term, because Re(MW) is a measurement of an average droplet radius so that it have some sensitivity to droplets growth even though the precipitation occurs; 2) the first term is a modulation term which can amplify rainfall information coming from Re(MW), because as discussed above, when precipitation occurs the ratio will be greater than 1. Therefore Re(DI) is expected to be capable of the drizzle detection.

Using Eq.(2), the Re(DI) can be further expressed as:

$$\mathrm{Re}(DI) = \frac{LWP(MW)}{LWP(SR)} \cdot \mathrm{Re}(MW) \quad \text{(4-a)}$$

or $$\mathrm{Re}(DI) = \frac{LWP^2(MW)}{\tau^2 \cdot \mathrm{Re}(SR)} \quad \text{(4-b)}$$

where LWP(MW) is liquid water path derived from microwave measurement and LWP(SR) is LWP inferred from τ and Re(SR) with Eq.(2).

Now, we have three different forms of effective radius: Re(SR), Re(MW) and Re(DI). To better understand what different behaviors and different physical meanings they have in cloud formation and precipitation stages, we used radiative transfer models [SBDART model (Ricchiazzi et al., 1998) for visible/infrared, and MWRT model (Liu, 1998) for microwave] to do the following simulations. In each simulation, we assume a uniform profile of the cloud optical depth τ but a linearly increasing (or decreasing) profile of effective radius. Fig.2 shows LWP(SR) vs. LWP(MW). Note that the ratio of LWP(MW) to LWP(SR) equals to the ratio of Re(MW) to Re(SR) [ref. Eq.(3) and Eq.(4a)], we have:

1) When Re is vertically uniform (open circles in both Figs.2a and 2b), the ratio term LWP(MW)/LWP(SR)=1. When Re increases with height (Fig.2a), the ratio<1. When Re decreases with height (Fig.2b), the ratio>1.

2) For the same Re profile, the absolute difference between LWP(MW) and LWP(SR) increases with τ (or LWP) in both Figs.2a and 2b, but the ratio for Re-increasing profiles (Fig.2a) doesn't change as much as that for Re-decreasing profiles (Fig.2b).

3) For different Re profiles but the same LWP, in Fig.2a the ratio is almost constant no matter in what rate the Re increases with height, and points closely locate along the fitting function $Y=1.62X^{1.2}$, but in Fig.2b the points are substantially apart from each other.

The reasons lie in:

1) When effective radius varies linearly with the height, the average effective radius Re(avg) can be obtained by:

$$\begin{cases} \mathrm{Re}(avg) \approx \mathrm{Re}(top)/2 & if\ increses \\ \mathrm{Re}(avg) = (1+\alpha)\,\mathrm{Re}(top)/2 & if\ decreses \end{cases}$$

Where, α = Re(btm)/Re(top), Re(top) and Re(btm) are the effective radius at the top and bottom of cloud respectively.

2) Re(SR) is a proxy of effective radius at a level near the cloud top. How far away this level from the cloud top depends on the cloud optical depth; the smaller the τ is, the deeper into the cloud. On the other hand, Re(MW) is a good approximation of Re(avg). Therefore, for Re-increasing profiles, the ratios are in the range of (0.5,1) slightly depending on τ. For the Re-decreasing profiles, the ratio > 1 and the lager the α (or τ) is, the bigger the ratio will be.

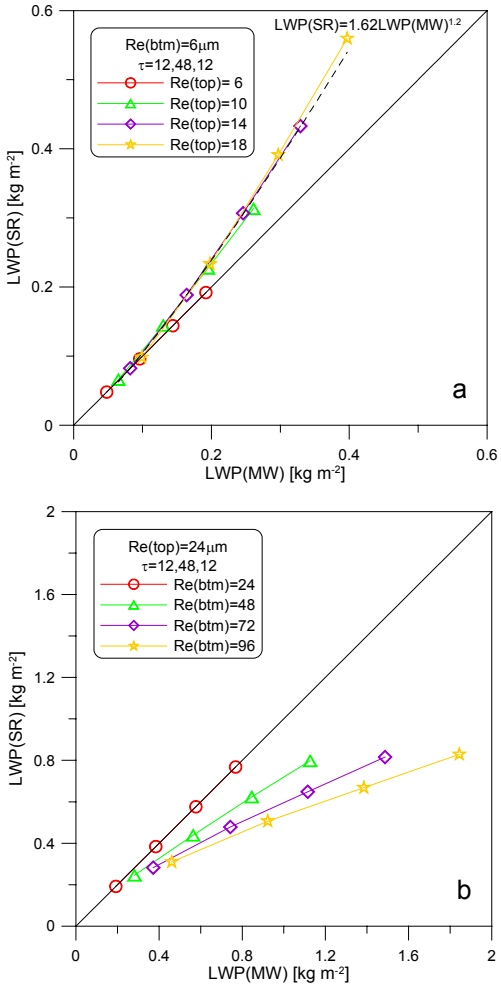

Fig.2 Computed LWP(SR) vs. LWP(MW) with τ varying from 12 to 48 with a step of 12, (a) when Re linearly increasing with height, and (b) when Re linearly decreasing with height. Profiles of Re are given by the Re(top) and Re(btm) which donate Res at the top and the bottom of the cloud, respectively. Also shown the best fit for the Re-increasing case (dash line).

Figure 3 shows the vertical locations at which Re(SR), Re(MW) and Re(DI) correspond to the effective radii. It also shows how the ratio term varies profile by profile at τ=36.

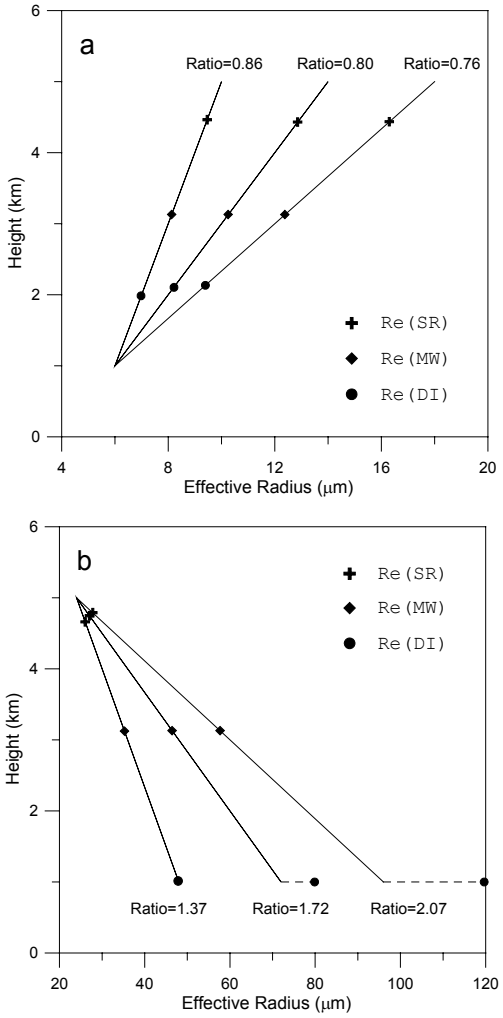

Fig.3 Illustration of the vertical locations at which Re(SR), Re(MW) and Re(DI) correspond to the effective radii at τ=36. The Re profiles are same as Fig2. (a) for Re-increasing case, (b) for Re-decreasing case. Also shown is the ratio for each profile.

3. CASE STUDY

VIRS and TMI Data from the Tropical Rainfall Measurement Mission (TRMM) satellite are used in this study. The reflectances at 0.63 μm and 1.61 μm VIRS channels are used to retrieve cloud optical depth and effective radius at the solar wavelengths. A new microwave algorithm is developed to derive cloud liquid water path LWP(MW) from 19 and 37 GHz frequencies. Since TMI has larger footprints than VIRS, the VIRS cloud retrievals are convolved with the TMI antenna pattern function to produce new VIRS pixels with the same footprint size of TMI's. Thus they are collocated with the actual TMI pixels. To avoid beam-filling error, only completely overcast pixels are selected. Additionally, pixels with cloud top temperature colder than 273 K are excluded in the analysis to avoid ice scattering.

Two cases were chosen for the case study. In Fig.4, the VIRS channel 4 image shows two clusters of stratiform cloud with a uniform warm cloud-top temperature (green color) over the Bay of Bengal at 09:30 UTC, 21 February 1999. And the vertically integrated rainrate from TRMM PR (Fig.5) shows that the case2 was associated with moderate rain but in the area of case1 there was no appreciable rainfall signal. It should be mentioned here that the possibility of the light rainfall, i.e. drizzle, cannot be excluded because drizzle signal is lower than the minimum detectable radar reflectivity factor 17dBZ.

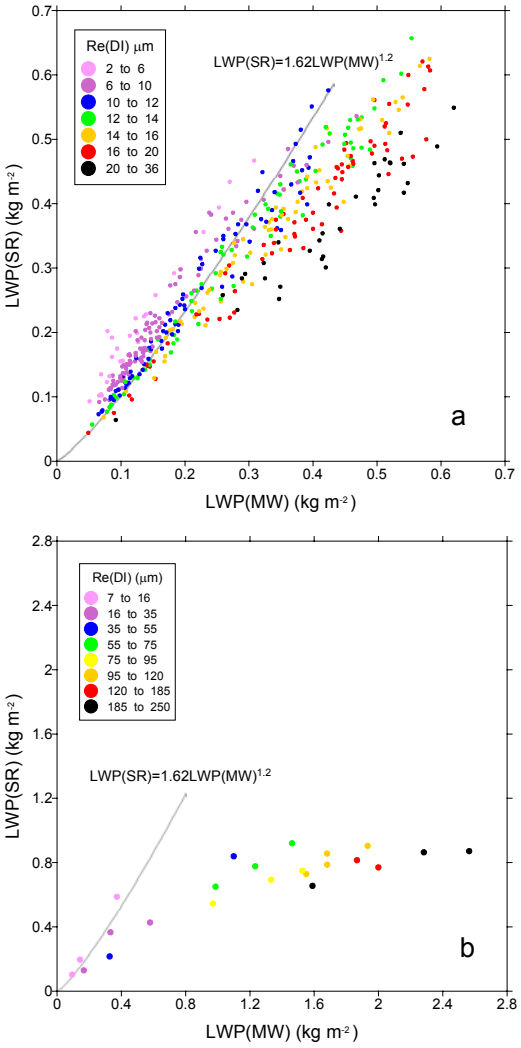

Fig.6 Shows the scatter diagram of LWPs retrieved from TMI and VIRS measurements with the classified Re(DI). (a) for the drizzle case, (b) for moderate rain case. A fitting line as discussed in section 2, $LWP(SR)=1.62LWP(MW)^{1.2}$, is also indicated

Figure 6 shows the scatter diagram of LWPs retrieved from TMI and VIRS measurements with the classified Re(DI). A fitting line as discussed in section 2, $LWP(SR)=1.62LWP(MW)^{1.2}$, is also indicated in the figures. The results are summarized as follows:

1) Below $LWP(MW)=0.2kgm^{-2}$, which is usually the critical value for stratocumulus to precipitate, points scatter along the fitting line. Above $LWP(MW)=0.2kgm^{-2}$ points deviate from the fitting line and bend to higher LWP(MW). These behaviors are consistent well with the model simulations given in the Fig.2. In the Fig.6b the LWP(SR) leveled off around $LWP(SR)=0.8kgm^{-2}$, the similar character being indicated by the model simulation at Re(top)=24μm (Fig.2b).

2) When Re(DI)>10μm nearly all the points are at the right side of the fitting line and at Re(DI)=10μm points scatter around the fitting line. It suggests that Re(DI)=10μm is a threshold for precipitation. Because for the most clouds the ratio of Re(MW) to Re(SR) is ~0.8 (Masunaga, 2001) [also shown in Fig.3a], this threshold is consistent with the threshold of Re(SR) ~ 15μm, which is often cited as the precipitation threshold in previous studies (Rosenfeld, 2000).

3) Since Re(DI) keeps increasing as the points bend to higher LWP(MW), Re(DI) may have capability to estimate rainrate, in particular the rainrate of drizzles, whose signal is too weak to be detected by TRMM PR. Fig.7 shows the Re(DI), Re(MW) and Re(SR) as a function of vertically integrated rainrate within a TMI pixel. Also shown the correlation coefficient between rain rate and these effective radii.

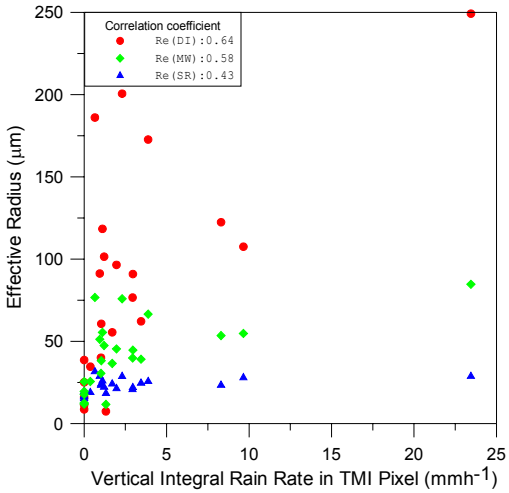

Fig.7 Re(DI), Re(MW) and Re(SR) as a function of vertical rain rate for the case2. Also shown correlation coefficient between the rain rate and Res (in legend).

From Fig.7, it shows:

1) When rainrate > 0, the Re(DI) increases with rainrate in a greater pace than the other two Res due to the amplification factor Re(MW)/Re(SR). As a result, its correlation with rainrate is greater than the other two.

2) At the rainrate = 0, points are congested and overlapped. It indicates that while the precipitation information is amplified in Re(DI) with the scale proportional to the rainrate but the precipitation threshold is not.

4. SUMMARY AND CONCLUSIONS

In this paper, we introduced a scaled effective radius as a drizzle index. Based on model simulations and analysis of TRMM satellite data, we demonstrated that this index is capable to infer both cloud microstructure and precipitation over a large area. The conclusions can be summarized as follows:

1) While Re(SR) is an estimation of the effective radius somewhere near the cloud top and Re(MW) is average effective radius over the whole cloud layer, Re(DI) represents the effective radius at the lower portion of the cloud layer.

2) For non-precipitating clouds with LWP < 0.2 kg m^{-2}, the ratio of Re(MW) to Re(SR) ranges from 0.85 to 1 and is insensitive to the rate at which Re increases with the height. For precipitating clouds, the ratio of Re(MW) to Re(SR) is greater than 1 and is positively correlated with rainrate.

3) Modulated by the ratio of Re(MW) to Re(SR), the scaled Re, Re(DI), has a greater sensitivity to precipitation.

References

Hansen, J.E., and L.D. Travis 1974. Light scattering in planetary atmospheres. *Space Sci. Rev.* **16**, 527-610

Ricchiazzi, P, S. Yang, C. Gautier, and D. Sowle, 1998: SBDART: A research and teaching software tool for plane-parallel radiative transfer in the Earth's atmosphere, *Bull. Amer. Meteor. Soc.*, **79**, 2101-2114.

Liu, G., 1998: A fast and accurate model for microwave radiance calculations. *J. Meteor. Soc. Japan,* **76**, 335-343.

Masunaga, H., T. Y. Nakajima, T. Nakajima, M. Kachi, R. Oki, and S. Kuroda, 2001: Physical Properties of Maritime Low Clouds as Retrieved by Combined Use of TRMM Microwave Imager and Visible/Infrared Scanner. I. Algorithm, *J. Geophys. Res.*, (Paper I)

Rosenfeld , D., 2000: Suppression of rain and snow by urban and industrial air pollution, *Science*, 287, 1793-1796.

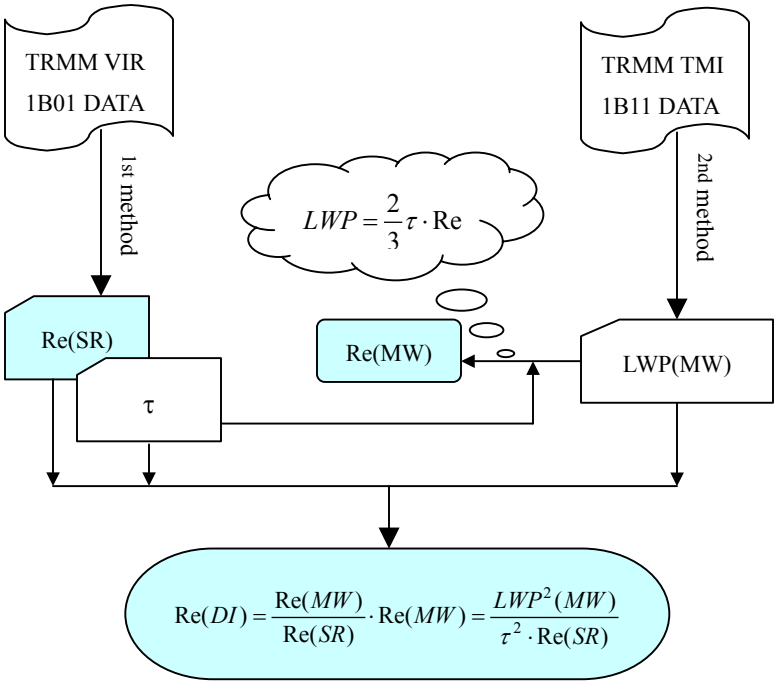

Figure 1 The scheme to compute the Re(SR), Re(MW) and Re(DI) and their relationship

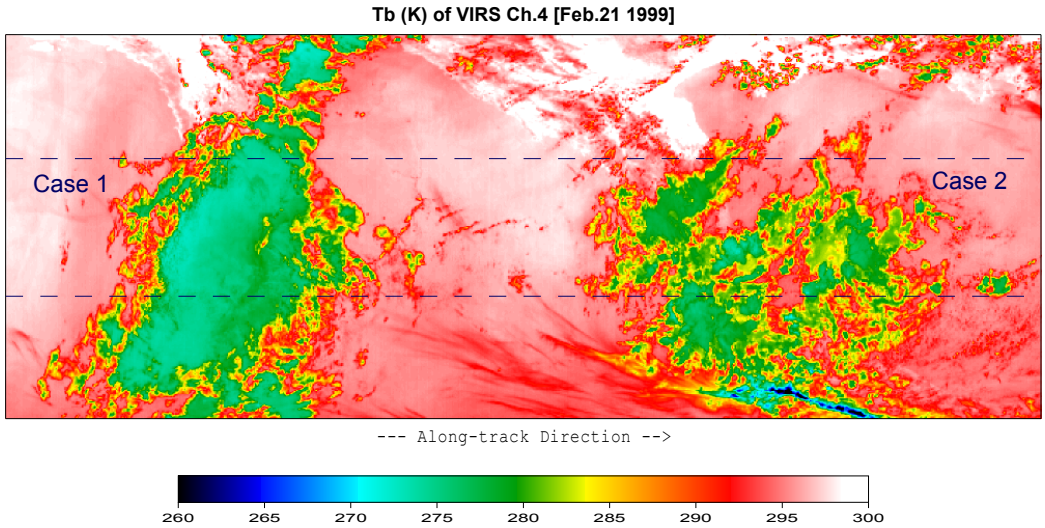

Figure 4 TRMM VIRS channel 4 Image at 09:30 UTC on 21 February 1999, showing two clusters of stratiform cloud with a uniform warm cloud-top temperature (green color) over the Bay of Bengal. *The two parallel dash lines delimit the 230 km PR swath. The swath is oriented northwest to southeast.*

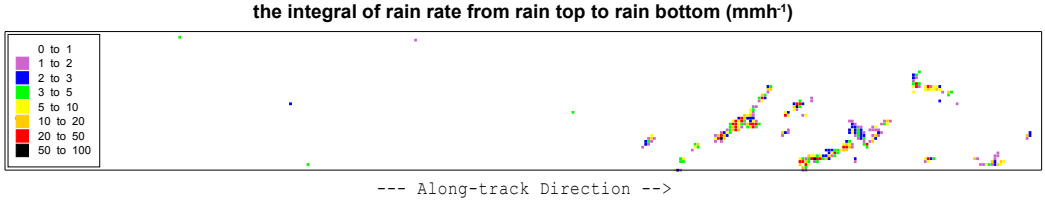

Figure 5 Spatial distribution of vertically integrated rainrate along the PR swath. Same time as in Fig.4